Imputing missing RNA-seq data from DNA methylation by using transfer learning based-deep neural network

Xiang Zhou[1], Hua Chai[1], Huiying Zhao[2], Ching-Hsing Luo[1]*, and Yuedong Yang[1,3]*

[1]School of Data and Computer Science, Sun Yat-sen University, Guangzhou, China, [2]Sun Yat-sen Memorial Hospital, Sun Yat-sen University, Guangzhou, China, [3]Key Laboratory of Machine Intelligence and Advanced Computing (Sun Yat-sen University), Ministry of Education, China

* yangyd25@mail.sysu.edu.cn; luojinx5@mail.sysu.edu.cn

Abstract

Multi-omics integrative analysis can capture the associations of different omics and thus provides a comprehensive view of the complex mechanisms in cancers. However, it is common that one portion of samples miss one type of omics data due to various limitations in experiments, which can be an obstacle for downstream analysis where complete dataset is needed. Current imputation methods mainly focus on single cancer dataset, which are limited by their ability to capture information from large pan-cancer dataset. We present a novel transfer learning-based deep neural network to impute missing gene expression data from DNA methylation data, namely TDimpute. The pan-cancer dataset was utilized to train a general model for all cancers, which was then fine-tuned on each cancer dataset for the specific cancer. We compared our method to other state-of-the-art methods on 16 cancer datasets, and found that our method consistently outperforms other methods in terms of imputation error, methylation-expression correlations recovery, and downstream analysis including the identification of DNA methylation-driving genes and prognosis-related genes, clustering analysis, and survival analysis. The improvements are especially pronounced at high missing rates.

Author summary

As an epigenetic modification, DNA methylation plays an important role in regulating gene expression. However, due to limitations of sample availability and cost, some samples aren't measured with gene expression, which results in a reduced sample size for integrative analysis of DNA methylation and gene expression. The accuracy of traditional imputation methods are limited since they cannot effectively utilize the information from DNA methylation data and other relevant datasets. With the power of modeling nonlinear relationship, we used deep neural network to impute missing gene expression data using the nonlinear transformation from DNA methylation data to gene expression data. We also employed transfer learning to alleviate the data insufficiency in training the deep leaning model. In 16 cancer datasets from The Cancer Genome Atlas (TCGA), our method yields higher accuracy compared to other methods. More importantly, better performance of the downstream analysis on imputed gene expression datasets are achieved, which indicates the missing data imputed by our method are more biologically meaningful.

Introduction

Recent development of molecular biology and high-throughput technologies facilitates the simultaneous measurement of various biological omics data such as genomics, transcriptomics, epigenetics, proteomics, and metabolomics for a single patient. Compared with single-omics analysis, integrative analysis of multi-omics data provides comprehensive insights of cancer occurrence and progression, and thus strengthens our ability to predict cancer

prognosis and to discover various levels of biomarker. However, due to technical limitations of experimental settings or high costs for acquiring the omics data, most samples aren't measured with all types of omics data, and lack one part of omics types (called "block missing"). This problem is prevalent in publicly available multi-omics dataset, such as The Cancer Genome Atlas (TCGA). In traditional multi-omics integration studies, samples with missing omics are usually removed, which greatly reduces the sample size, especially when concatenating many types of omics data [1].

When the data is missing at random in single omics data, many methods have been proposed for imputing the missing values by using correlation structure among matrix entries, such as singular value decomposition imputation (SVD), k-nearest neighbor (KNN) [2]. However, these traditional methods may not be suitable for the cases lacking a whole set of features. In order to address this issue, several methods have been specifically designed. Voillet et al. used multiple hot-deck imputation approach to impute missing rows in multi-omics dataset for multiple factor analysis [3]. To improve the reliability of gene network inference, Imbert et al. used multiple hot-deck imputation method to process RNA-seq data with missing rows, where they measured the similarities to cases in a standard database, and fixed the missing values according to the case with the highest similarity [4]. Obviously, this way to use only the most similar case (neighbor) might be unstable due to random fluctuations in its neighbors. Recently, Dong *et al.* proposed a k-nearest neighbor weighted method (named as TOBMI by the authors) to impute mRNA-missing samples through evaluating the sample similarity by DNA methylation data [5]. However, TOBMI suffers from poor scalability for dataset with large sample size and high dimensionality, and the accuracy is still limited since the size of specific cancer dataset is relatively small. More importantly, it cannot capture information from other related cancer datasets.

In recent years, deep neural network has demonstrated its superiority on modeling complex nonlinear relationships and enjoys scalability and flexibility. One or multiple hidden layers and nonlinear activation function are employed to capture the nonlinear patterns between input and output data. For the gene expression imputation or prediction, many deep learning models have been proposed. Chen *et al.* built a multilayer feedforward neural network to predict the expression of target genes from the expression of ~1000 landmark genes [6]. Xie *et al.* constructed a similar deep model to infer gene expression from genotypes of genetic variants [7]. Based on convolutional neural network, Zeng *et al.* used promoter sequences and enhancer-promoter correlations to predict gene expression [8]. With the ability to recover partially corrupted input data, denoising autoencoder (DAE) was used to impute missing values in single-cell RNA-seq data [9, 10]. Besides genetic variants and transcription factors, DNA methylation is another fundamental mechanism to regulate gene expression, and aberrant DNA methylation is considered as an important contributor to disease phenotypes (Gevaert, et al., 2015). Thus, gene expression imputation can improve the correlation analysis between methylation and gene expression, by increasing the sample size when expression data are not available. Nevertheless, the studies on predicting gene expression from DNA methylation are limited, and the only known one is TOBMI [5].

One obstacle for the application of these deep learning model to multi-omics dataset is the high dimensionality (>20,000 features) in omics data while a small sample size. Even the TCGA has only hundreds of samples for each cancer type. Thus, it is hard to train an accurate model with millions of parameters in deep learning architecture. In such scenarios, transfer learning is usually considered as a promising method, where parameters trained for a task with large amount of data are reused as the initialization parameters for a similar task with limited data [11]. The transfer learning has been widely used in the computer vision including object detection [12], image segmentation [13].

For the omics data analysis of cancers, the transfer learning strategy has been applied to different tasks. Li *et al.* built a pan-cancer Cox model for the prediction of survival time, where eight cancer types were combined to assist the training of target cancer dataset [11]. Yousefi *et al.* used transfer learning approach to predict the clinical outcomes utilizing samples from uterine corpus endometrial carcinoma and ovarian serous carcinoma to augment target breast cancer dataset to improve the prediction of clinical outcomes [14]. Hajiramezanali *et al.* learned information from the Head and Neck Squamous Cell Carcinoma cancer to subtype lung cancer [15]. Based on the assumption that different types of cancer may share common mechanisms [16, 17], transfer learning is becoming a useful approach for the prediction of missing data by learning from the data of different cancer types.

Imputing RNA-seq data by TDimpute

Schematic overview of TDimpute
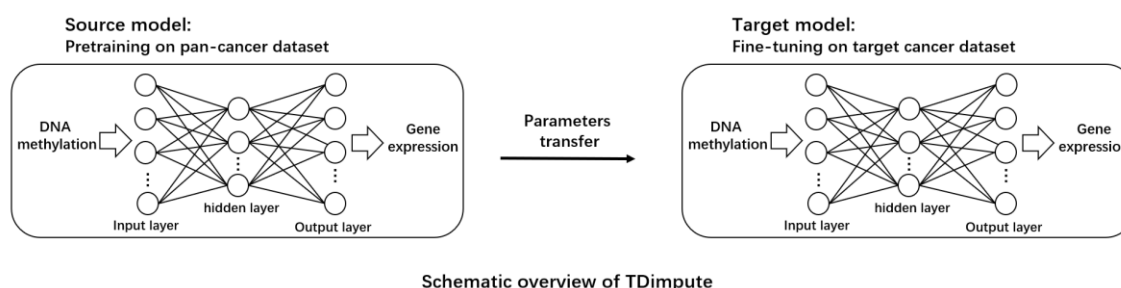
Fig 1. The architecture of transfer learning based deep neural network (TDimpute) for imputing missing gene expression values in multi-omics dataset. The deep neural network: DNA methylation data are transformed into gene expression data and the root mean squared error (RMSE) between the actual output and desired output is minimized. Transfer learning: pan-cancer dataset is used to train the general imputation model for pan cancers, which is specifically tuned for each type of cancer.

In this study, we propose a transfer learning based deep neural network method for imputing gene expression from DNA methylation data, namely TDimpute. Specifically, we first train a deep neural network on the pan-cancer dataset to build a general imputation model for all cancers, which is then transferred to target cancer types (see Fig 1 for a schematic overview). To the best of our knowledge, this is the first time to employ the transfer deep learning for the imputation of gene expression from methylation. The method was tested to recover gene expressions for 16 cancer types at five different missing rates, and achieved better performances than other methods by measurement of the root mean square errors (RMSE) and Pearson correlation coefficients to actual values. We further evaluated the imputed gene expressions for the identification of methylation-driving genes, prognosis-related genes, clustering analysis, and survival analysis. The results show that our method consistently provides the best performances. These results confirm that TDimpute succeeds in transferring related information from pan-cancer data to target cancer data.

Results

## Comparisons on the imputation accuracy

We evaluated the imputation accuracy of 6 imputation methods by the average root mean square errors (RMSE) across 16 cancer datasets over different missing rates. The missing rate means the fraction of samples whose gene expression data are removed. As shown in Fig 2A, TOBMI achieves similar but consistently lower RMSE than SVD. SVD has a slow increase of RMSE from 1.06 to 1.01 when missing rates change from 10% to 70%, but then a sharp increase to 1.24 that is even worse than the result by the Mean method. Overall, the Mean method has the worst performance, which is consistent with the trend in the original paper [5]. By comparison, TDimpute-self without using transfer learning yields 6%-12% lower RMSE than TOBMI at different missing rates. TDimpute-noTF, as a general model, is trained on the pan-cancer dataset (excluding the target cancer). The model doesn't use information from the target cancer and thus shows a constant performance. It doesn't perform well but better than the Mean method. The performance is even better than SVD and TOBMI when the missing rate is above 70%. TDimpute, a further transfer learning of the target cancer from TDimpute-noTF, decreases the RMSE by 7%-16% over TDimpute-noTF. The RMSE by TDimpute is also 2%-5% lower than TDimpute-self with a bigger difference at a higher missing rate. These results confirm the power of our TDimpute method in transferring knowledge from the other cancer types to improve the imputation performance. We also noted SVD, MI hot-deck, and TOBMI have close to constant RMSE values for missing rates 70% and 10%, indicating that 3 times increase of sample sizes don't contribute much to increase the imputation accuracy. Instead, deep learning methods, TDimpute and TDimpute-self, decrease the RMSE by 5% and 7%, respectively, indicating the ability of further improvement with an increase of sample size in future.

When measured by the squared correlation (R^2) between the imputed and actual values by each sample (Fig 2B), TDimpute is consistently the best, followed by the TDimput-self. Differently, SVD ranks the 3rd except at a missing rate of 90%, where SVD has the lowest R^2 of 0.909. The Mean imputation keeps the lowest performance. Hereafter, we will focus on the comparison with SVD and TOBMI methods.
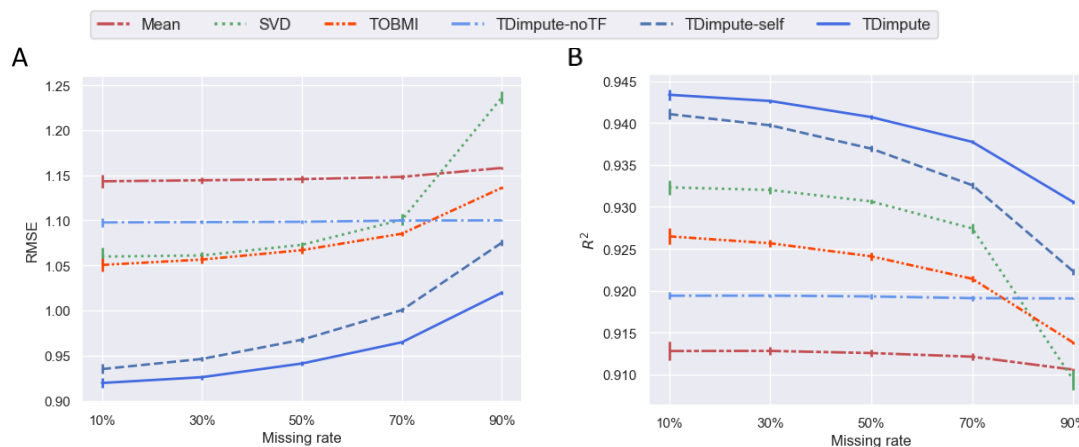
Fig 2. Imputation accuracy of each imputation method. Results were averaged across 16 imputed cancer datasets. (**A**) RMSE values of each method. (**B**) The squared Pearson correlation coefficient (R^2) between each sample of the imputed data and the original full data. TDimpute-self indicates the TDimpute trained and predicted on the target cancer dataset. TDimpute-noTF indicates the TDimpute trained on the pan-cancer dataset (excluding the target cancer) and predicted on the target cancer dataset. The standard deviations are shown with error bars.

Impact on the methylation-expression correlations and the identification of methylation-driving genes
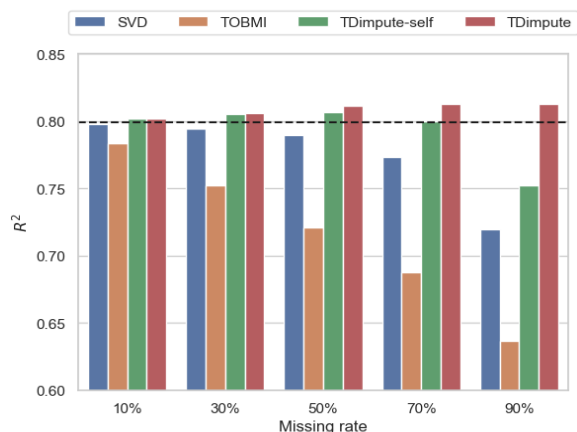
Fig 3. The average correlations R^2 of top 100 CpG-gene pairs over 16 cancer datasets by four imputed methods. Dashed black line is the correlations from the actual dataset.

Table 1. The average PR-AUC over 16 cancers for recovering methylation-driving genes according to the imputed relative to the actual gene expression data. Average performance across 16 imputed cancer datasets are reported. Best results are highlighted in bold face. * indicates statistical significance (p-value < 0.05) between TDimpute and other three methods (SVD, TOBMI, TDimpute-self).

Missing rate	SVD	TOBMI	TDimpute-self	TDimpute
10%	0.988*	0.988*	0.992*	**0.993**
30%	0.954*	0.956*	0.969*	**0.974**
50%	0.900*	0.898*	0.932*	**0.943**
70%	0.818*	0.807*	0.867*	**0.892**
90%	0.665*	0.651*	0.712*	**0.788**

For multi-omics dataset, proper imputation method should preserve the correlation structures between different types of omics. Since the most correlated CpG-gene pairs play the most important roles, we only compare the impact of imputation methods by the average R^2 of top 100 CpG-gene pairs from full datasets. As shown in Fig 3, TOBMI displays a dramatic decrease of R^2 from 0.78 to 0.64 with the increase of missing rates. SVD method has a small decrease of R^2 from 0.80 to 0.79 when missing rates increase from 10% to 50%, but a large drop to 0.72 at a missing rate of 90%. In contrast, both TDimpute and TDimpute-self have R^2 values fluctuating around the ideal values (R^2=0.8) when missing rates are less than 70%. At a missing rate of 90%, TDimpute-self by using single dataset has a drop of R^2 to 0.75, while TDimpute doesn't show any decrease. This is as expected because transfer learning has been widely proven to solve the problem of small sample sizes.

We further investigate whether the preservation of correlations can obtain better performance in the identification of methylation-driving genes. The performance is evaluated by PR-AUC and the overlap of top 100 methylation-driving gene from imputed and full datasets. A higher value means stronger

concordance with the gene list identified from actual dataset. Tables 1 and S3.1 show that our proposed TDimpute method has the highest PR-AUC values and overlap with true methylation-driving genes among the four methods across different missing rates. TDimpute-self ranks the second in selecting methylation-driving genes, followed by SVD and TOBMI. Compared with SVD, TDimpute achieves 0.5%-19% improvement for PR-AUC, and 3%-103% improvement for overlapped genes. The improvement is especially pronounced at high missing rates.

Impact on the identification of prognosis-related genes

Table 2. The average PR-AUC for recovering prognosis-related genes according to the imputed relative to the actual gene expression data. The * indicates there is a significant difference from the results by TDimpute by paired T-test.

Missing rate	SVD	TOBMI	TDimpute-self	TDimpute
10%	0.856*	0.866*	0.876*	**0.880**
30%	0.674*	0.709*	0.727*	**0.742**
50%	0.532*	0.566*	0.594*	**0.617**
70%	0.404*	0.429*	0.460*	**0.494**
90%	0.275*	0.277*	0.295*	**0.357**

Table 3. The average enrichment factors of top 100 prognosis-related genes overlapped with the genes collected in the Human Protein Atlas. The * indicates there is a significant difference from the results by TDimpute by paired T-test.

Missing rate	SVD	TOBMI	TDimpute-self	TDimpute
10%	5.53*	5.83	5.71	**5.91**
30%	3.46*	4.08	4.22	**4.25**
50%	2.08*	2.74	2.94	**3.06**
70%	1.14*	1.60*	1.87	**2.03**
90%	0.56*	0.47*	0.89*	**1.14**

We investigated the recovery power of different imputation methods on the identification of significantly prognosis-related genes. To evaluate the selected genes, we compared the genes identified from the imputed to those from the actual data. Consistent with the performance in the imputation accuracy, Tables 2 and S5.1 show that TDimpute method achieves 2%-28% higher PR-AUC values, and 4%-54% more number of overlapped genes than those by the TOBMI method. TOBMI and SVD achieve the lowest values, with TOBMI performing slightly better than SVD. We also investigate the enrichment of the top 100 genes overlapped with the prognosis-related gene list downloaded from The Human Protein Atlas [18] relative to the random. Table 3 demonstrates that TDimpute achieves the largest enrichment factors, indicating its ability to identify the really validated prognosis-related genes.

Impact on the performance of clustering analysis and survival analysis

We also evaluate the effects of different imputation methods on clustering analysis and survival analysis. By input of top 100 prognosis-related genes, K-means algorithm is used to divided the samples into two clusters. The adjusted rand index (ARI) for the clustering concordance is shown in Fig 4A. For all methods, accuracy decreases with increasing missing rates, which is consistent with the previous study [10]. As expected, TDimpute achieves the highest clustering concordance among the four imputation methods consistently under different missing rates.

A further survival analysis (Fig 4B) shows that TDimpute achieves the best C-index, followed by TDimpute-self, SVD method, and TOBMI method. Despite showing a worse performance in the imputation accuracy, SVD performs better than TOBMI in this evaluation metric. In addition, the C-index of TDimpute, TDimpute-self, and SVD are relatively robust to the missing rates compared to TOBMI that showed a 9% decrease in C-index with 90% of samples missing gene expression values.
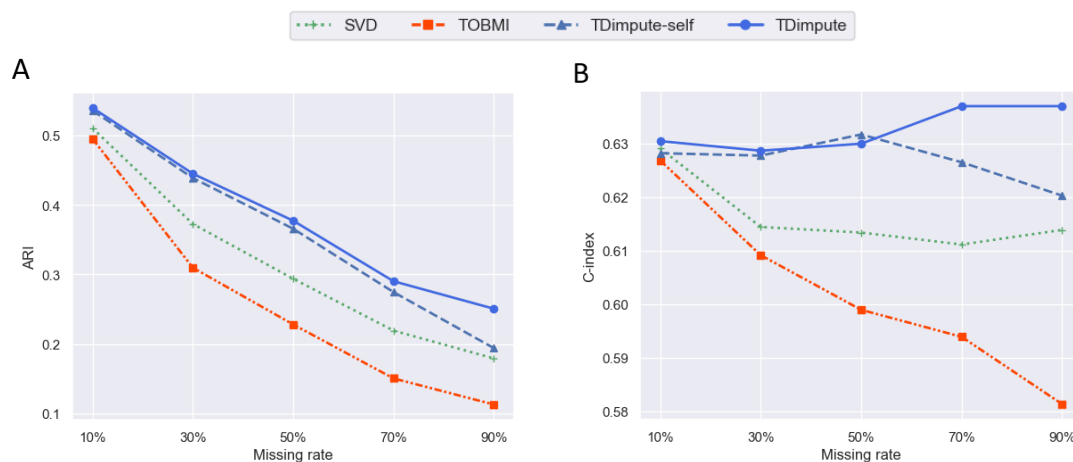
Fig 4. (A) The average adjusted rand index (ARI) of the clusters from the imputed and actual data, and **(B)** the average C-index by survival analyses based on imputed data over 16 cancers.

Real data application

We downloaded Uterine corpus endometrial carcinoma (UCEC) data from TCGA, and obtained 439 samples with methylation data. Among the samples with methylation data, only 172 samples have expression data at the same time. The samples with both expression and methylation data were considered as training dataset. For the top 100 prognosis-related genes identified from the dataset imputed by TDimpute, 26 genes (Table S7) were found in The Human Protein Atlas [18], corresponding to an enrichment factor of 3.05 (26/100/(1621/19027)). Among the 26 genes, 20 genes were previously reported to relevant to multiple types of cancer, of which 5 genes (TXN, UCHL1, GAL, CALCA, PEG10) connect to UCEC and 6 genes connect to gynecologic cancers (ovarian cancer and cervical cancer) and breast cancer.

K-means method is used to cluster the 439 samples after imputation, and two resulted clusters are used to plot the survival curve. The log-rank test was used to evaluate the difference in prognosis of each cluster. As shown in Fig 5, TDimpute achieves more significant difference between the two clusters, where the p-value is decreased from 0.0095 to 0.000173. SVD and TDimpute-self have similar results with TOBMI with P-values of 0.0012 and 0.0011, respectively. The survival analysis on the imputed dataset by TDimpute are also enhanced with the largest C-index of 0.588, compared to TDimpute-self, SVD, TOBMI with C-index of 0.575, 0.55, and 0.553, respectively.

For all the mentioned experiments, the results per cancer dataset are detailed in S1-S5 Figs, and S2-S6 Tables.
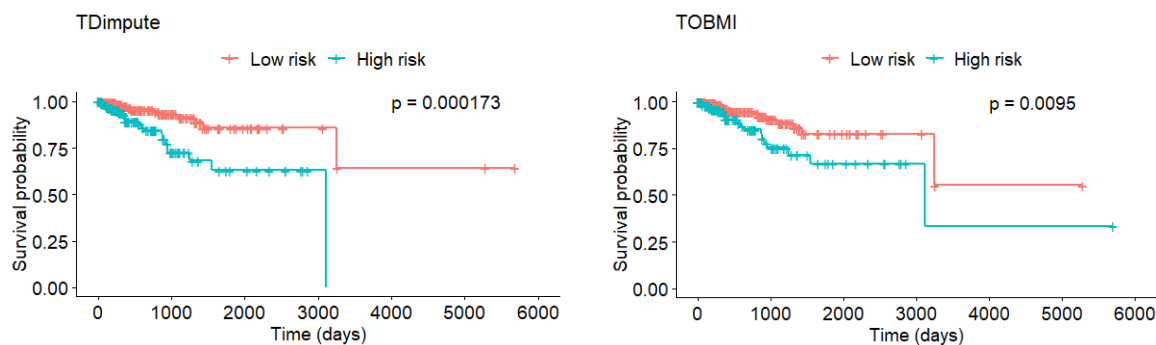
Fig 5. Kaplan-Meier plot for the two clusters obtained from the UCEC dataset imputed by TDimpute and TOBMI, respectively.

Discussion

Our TDimpute method is designed to impute multi-omics dataset where large, contiguous blocks of features (i.e., omics data) go missing at once. In this paper, TDimpute perform missing gene expression imputation by building a highly nonlinear mapping from DNA methylation data to gene expression data. Due to the limited size of cancer datasets in TCGA, we use transfer learning to capture the commonalties in pan-cancer dataset for parameter pre-training. We compare TDimpute with/without transfer learning, SVD and TOBMI method in imputation accuracy of RMSE and correlation R^2, methylation-expression correlations. Since the main task of imputation is to recover biologically meaningful gene expression data for downstream analysis, we also evaluate the imputation performance for the identification of methylation-driving gene, prognosis-related genes, clustering analysis and survival prediction. It is worthy to note that although only methylation and gene expression data are illustrated in this paper, our method is capable of incorporating other omics data by following a similar framework.

Experimental results on 16 cancer datasets confirm that our TDimpute method without transfer learning outperforms SVD and TOBMI method in different evaluation metrics. Based on transfer learning, our TDimpute method can further improve the performance especially at large missing rate. In addition, the ranking of SVD and TOBMI method by imputation accuracy (RMSE and correlation R^2) are not strictly correlated with their performance in preservation of methylation-expression correlation, clustering analysis and survival prediction, but our TDimpute method provide approximately consistent performance in downstream analysis.

Besides the outstanding performance of imputation accuracy and downstream analysis, another main benefit of our proposed methods is the computational efficiency and convenience. Based on GPU acceleration, our TDimpute method is capable of processing large-scale pan-cancer multi-omics dataset including tens of thousands of samples and hundreds of thousands of features, while TOBMI and SVD suffer poor scalability due to the computational complexity of distance matrix computation and singular value decomposition operations. Based on pre-trained model, transfer learning framework can also accelerate the training process on the target dataset. In addition, our deep neural network model only needs to be trained one time and the trained model can be applied directly to any new samples for imputation, while TOBMI and SVD are not model-based method and have to recompute the whole dataset when new samples are given. This is very convenient in practice.

Future work can focus on reducing the amount of model parameters and integrating more related training samples. Since we only use the correlation between omics for imputation, one possible direction is to leverage prior knowledge of gene-gene interaction network. The known relationships between variables/genes has demonstrated its ability to significantly reduce the model parameters by enforcing sparsity on the connections of neural network [19]. The performance of this approach is dependent on the quality of the gene-gene networks, and more investigation need to be done in this direction.

Methods

Datasets

We obtained the data for 33 cancer types from The Cancer Genome Atlas (TCGA) using the R package TCGA-assembler [20], including RNA-seq gene expression data (UNC IlluminaHiSeq_RNASeqV2), DNA methylation data (JHU-USC HumanMethylation450), and clinical information with follow-up. Originally, 20531 genes and 485577 methylation sites were collected. We excluded genes with zero values in the RNA-seq data across all samples. The remained 19027 genes were converted by the $\log_2(G + 1)$, where G is the raw gene expression value. For DNA methylation data, we excluded methylation sites with "NA" values, and 269023 methylation sites remain. By further removing sites with small variances (< 0.05) over all samples, 27717 CpG sites were kept. Here, for evaluating all imputing methods we kept only samples having both RNA-seq and DNA methylation data. Finally, the dataset contains 8856 samples with expression data for genes and methylation values for 33 cancers, namely pan-cancer dataset.

To keep enough sample size for model building, we only selected cancer types containing > 200 samples with complete DNA methylation, gene expression, and clinical data, leading to 16 cancer types for test: Breast adenocarcinoma (BRCA), Thyroid carcinoma (THCA), Brain lower grade glioma (LGG), head and neck squamous cell carcinoma (HNSC), Prostate adenocarcinoma (PRAD), Lung adenocarcinoma (LUAD), Skin cutaneous melanoma (SKCM), Bladder urothelial carcinoma (BLCA), Liver hepatocellular carcinoma (LIHC), Lung squamous cell carcinoma (LUSC), Skin cutaneous melanoma (STAD), Kidney renal clear cell carcinoma (KIRC), Cervical squamous cell carcinoma and endocervical adenocarcinoma (CESC), Kidney renal papillary cell carcinoma (KIRP), Colon carcinoma (COAD), and Sarcoma (SARC). The cancer types and their sample sizes are detailed in Table S1.

The architecture of our imputation method

Deep neural network was employed for imputing missing gene expression values from the DNA methylation. To expand the sample size for training the model, we leverage the pan-cancer dataset to generate a model for all cancer types. Then, the model is fine-tuned respectively on each cancer type to obtain specific models.

Deep neural network architecture. As shown in Fig 1, the deep neural network includes input layer, output layer, and one or multiple hidden layers. The nodes between layers are fully connected. Here, we use x^0 to represent the input of network, and the output vector x^l at lth layer can be formulated as

$$x^l = f(W^l x^{l-1} + b^l) \qquad (1)$$

where x^{l-1} denotes the output of previous layer $l-1$, $f(\cdot)$ is the activation function such as the sigmoid and Relu functions, and W and b are weight matrix and bias vector, respectively. W and b are parameters that need to be learned.

The loss function for training is the root mean squared error (RMSE):

$$L(y, y^0) = \sqrt{\frac{1}{N}\sum_{i=1}^{N}(y_i - y_i^0)^2} \qquad (2)$$

where y_i^0 and y_i are the experimentally measured and predicted expression value for gene *i*, and N is the dimension of output vector (i.e., the number of genes). The network can be considered as a highly nonlinear regression function that maps DNA methylation data (input) to gene expression data (output).

Transfer learning-based models. To train the prediction model for one target cancer in the TCGA, the datasets of other cancer types are combined to generate a multi-cancer model that is then fine-tuned by the target cancer data (Fig 1). The data of the target cancer was excluded to train the multi-cancer model as we need to remove different portions of the data for the target cancer to evaluate our imputation model. A half number of epochs (300 relative to 150) during the fine-tune step was selected to avoid over-fitting over single cancer type.

Parameters setting. For our deep neural network, we selected the following hype-parameters: 1 hidden layer (selected from 1 and 3) including 4000 (from 500, 1000, 2000, and 4000), Sigmoid activation function (from Tanh, Relu, and Sigmoid), epochs of 100 (from 100, 150, 300, and 500), and batch size of 16 (from 16, 32, 64, and 128). Adam optimizer was used to optimize parameters. For the training of multi-cancer models, a batch size of 128 was used to train 300 epochs because of the bigger training set by using 32 cancers (150 epochs were used for fine-tuning stage). All hyperparameters were selected after test and trials for a low value of RMSE. All methods were implemented with TensorFlow. Dropout wasn't used as it decreased the performance.

Missing data simulation and other methods for comparison

To simulate the missing values in omics, we randomly selected increasing fractions (10%, 30%, 50%, 70%, 90%) of samples in the full dataset and remove their gene expression data. The samples with missing gene expression are set as testing dataset and the remaining samples with complete omics are set as training dataset. At each level of missing rate, we repeat this procedure 5 times to obtain a robust evaluation of each method and the averaged results are reported in all the following experiments. The original full dataset is referred as a gold standard for our comparisons. For TDimpute and SVD method, gene expression data are scaled to the range of [0, 1].

We compare our method with the Mean imputation method, TOBMI [5], and SVD imputation method [2]. The default or suggested parameters were used for these methods.

Preservation of methylation-expression correlations and methylation-driving genes

Here, we use the squared Pearson correlation coefficient R^2 to evaluate the effect of imputation method on the correlations between DNA methylation and gene expression. Since one gene might be associated with multiple CpG sites, we only considered the CpG-gene pair with the strongest correlation in this paper. Based on the methylation-expression regulation, many studies have been conducted to identify cancer-related DNA methylation-driving (hyper and hypo methylated) genes [21]. Hence, we also evaluate the effect of imputation methods on the identification of methylation-driving genes. We define the methylation-driving genes (i.e., significantly correlated CpG-gene pairs) with the $R^2 \geq 0.5$ and FDR-$q \leq 0.05$. The pairs with R^2 greater than a threshold are considered to be correlated, according to which we can obtain the area under precision-recall curve (PR-AUC). We also computed the overlap between the top 100 ranked genes identified from imputed datasets and the original full datasets.

Preservation of prognosis-related genes

A common task in the analysis of gene expression data is the identification of prognostic genes. In order to evaluate the effect of different imputation method on the identification of potentially prognosis-related gene, we build univariate Cox proportional hazard regression models to select statistically significant genes correlated with overall survivals. With the Cox model, each gene is assigned a p-value describing the significance of the relation between the gene and a target cancer. The prognosis-related genes are identified with p-value ≤ 0.05. We rank the genes by their p-values, and evaluate the consistency between the gene lists from imputed datasets and the original full datasets using PR-AUC and the overlapped top 100 ranked genes.

To validate our gene rankings with independent information, we download the list of prognosis-related genes from The Human Protein Atlas (THPA) [18], and compare the enrichment factors of the top 100 ranked genes in the list from THPA. The enrichment factor is calculated with $EF = (N_{\text{True}}/N_{\text{selected}})/(N_{\text{Active}}/N_{\text{Total}})$, where N_{True} is the number of true positives, N_{selected} is the number of top k selected genes, N_{Active} and N_{Total} are the number of prognosis-related genes and total number of genes in THPA, respectively.

Impact on clustering analysis and survival analysis

We evaluated the relation of genes to cancer survivals by p-values output from the univariate Cox model. By using the top 100 genes, their expression values were used to divided samples into 2 clusters by the K-means. The clustering performance was assessed by adjusted rand index (ARI), which is a measure of agreement between the predicted cluster labels (on imputed dataset) and the true cluster labels (on original full dataset). We further made

survival prediction with significantly related genes ($p \leq 0.05$) by using the ridge regression regularized Cox model. Here, the glmnet package [22] in R was used for model construction, which is suitable for fitting regression model with high-dimensional data. The performance of the Cox model was assessed by the Harrell's concordance index (C-index) that measures the concordance between predicted survival risks and actual survival times. We used 5-fold cross validation (CV) to evaluate the performance.

Supporting information

S1 Fig. RMSE on 16 imputed cancer datasets with different missing rates.
(TIF)

S2 Fig. The squared Pearson correlation coefficients R^2 between each sample of the imputed data and the original full data on 16 imputed cancer datasets with different missing rates.
(TIF)

S3 Fig. The squared Pearson correlation coefficients R^2 between gene expression and methylation sites on 16 imputed cancer datasets with different missing rates.
(TIF)

S4 Fig. ARI on 16 imputed cancer datasets with different missing rates.
(TIF)

S5 Fig. C-index on 16 imputed cancer datasets with different missing rates.
(TIF)

S1 Table. The TCGA cancer types and their sample sizes used for test.
(XLSX)

S2 Table. PR-AUC for detecting methylation-driving genes on imputed cancer datasets over 16 cancer types.
(XLSX)

S3.1 Table. Overlap of top 100 methylation-driving genes from imputed dataset and full dataset.
(XLSX)

S3.2 Table. Overlap of top 100 methylation-driving genes between imputed dataset and full dataset over 16 cancer types.
(XLSX)

S4 Table. PR-AUC for detecting significantly prognostic gene on imputed datasets over 16 cancer types.
(XLSX)

S5.1 Table. Overlap of top 100 significantly prognostic genes identified by univariate Cox model between imputed datasets and full datasets.
(XLSX)

S5.2 Table. Overlap of top 100 prognostic genes identified by univariate Cox model between imputed dataset and full dataset over 16 cancer types.
(XLSX)

S6 Table. The enrichment factors of the top 100 ranked genes in the gene list from The Human Protein Atlas across 16 cancer types.
(XLSX)

S7 Table. The 26 genes validated in The Human Protein Atlas.
(XLSX)

Acknowledgements

References

1. Rappoport N, Shamir R. NEMO: Cancer subtyping by integration of partial multi-omic data. Bioinformatics. 2019. doi: 10.1093/bioinformatics/btz058 PMID: 30698637.

2. Troyanskaya O, Cantor M, Sherlock G, Brown P, Hastie T, Tibshirani R, et al. Missing value estimation methods for DNA microarrays. Bioinformatics. 2001;17(6):520-525.

3. Voillet V, Besse P, Liaubet L, San Cristobal M, Gonzalez I. Handling missing rows in multi-omics data integration: multiple imputation in multiple factor analysis framework. BMC Bioinformatics. 2016;17(1):402. doi: 10.1186/s12859-016-1273-5 PMID: 27716030.

4. Imbert A, Valsesia A, Le Gall C, Armenise C, Lefebvre G, Gourraud PA, et al. Multiple hot-deck imputation for network inference from RNA sequencing data. Bioinformatics. 2018;34(10):1726-1732. doi: 10.1093/bioinformatics/btx819 PMID: 29280999.

5. Dong X, Lin L, Zhang R, Zhao Y, Christiani DC, Wei Y, et al. TOBMI: Trans-omics block missing data imputation using a k-Nearest Neighbor weighted approach. Bioinformatics. 2018;35(8):1278-1283. doi: 10.1093/bioinformatics/bty796 PMID: 30202885.

6. Chen Y, Li Y, Narayan R, Subramanian A, Xie X. Gene expression inference with deep learning. Bioinformatics. 2016;32(12):1832-9. doi: 10.1093/bioinformatics/btw074 PMID: 26873929.

7. Xie R, Wen J, Quitadamo A, Cheng J, Shi X. A deep auto-encoder model for gene expression prediction. BMC Genomics. 2017;18(Suppl 9):845. doi: 10.1186/s12864-017-4226-0 PMID: 29219072.

8. Zeng W, Wang Y, Jiang R. Integrating distal and proximal information to predict gene expression via a densely connected convolutional neural network. Bioinformatics. 2019. doi: 10.1093/bioinformatics/btz562 PMID: 31318408.

9. Eraslan G, Simon LM, Mircea M, Mueller NS, Theis FJ. Single-cell RNA-seq denoising using a deep count autoencoder. Nat Commun. 2019;10(1):390. doi: 10.1038/s41467-018-07931-2 PMID: 30674886.

10. Tian T, Wan J, Song Q, Wei Z. Clustering single-cell RNA-seq data with a model-based deep learning approach. Nature Machine Intelligence. 2019;1(4):191-198. doi: 10.1038/s42256-019-0037-0.

11. Li Y, Wang L, Wang J, Ye J, Reddy CK, editors. Transfer learning for survival analysis via efficient L2, 1-norm regularized Cox regression. 2016 IEEE 16th International Conference on Data Mining (ICDM); 2016: IEEE.

12. Girshick R, Donahue J, Darrell T, Malik J, editors. Rich feature hierarchies for accurate object detection and semantic segmentation. Proceedings of the IEEE conference on computer vision and pattern recognition; 2014.

13. He K, Gkioxari G, Dollár P, Girshick R, editors. Mask r-cnn. Proceedings of the IEEE international conference on computer vision; 2017.

14. Yousefi S, Amrollahi F, Amgad M, Dong C, Lewis JE, Song C, et al. Predicting clinical outcomes from large scale cancer genomic profiles with deep survival models. Sci Rep. 2017;7(1):11707. doi: 10.1038/s41598-017-11817-6 PMID: 28916782.

15. Hajiramezanali E, Dadaneh SZ, Karbalayghareh A, Zhou M, Qian X, editors. Bayesian multi-domain learning for cancer subtype discovery from next-generation sequencing count data. Advances in Neural Information Processing Systems; 2018.

16. Yang X, Gao L, Zhang S. Comparative pan-cancer DNA methylation analysis reveals cancer common and specific patterns. Brief Bioinform. 2017;18(5):761-773. doi: 10.1093/bib/bbw063 PMID: 27436122.

17. Hoadley KA, Yau C, Wolf DM, Cherniack AD, Tamborero D, Ng S, et al. Multiplatform analysis of 12 cancer types reveals molecular classification within and across tissues of origin. Cell. 2014;158(4):929-944. doi: 10.1016/j.cell.2014.06.049 PMID: 25109877.

18. Uhlen M, Zhang C, Lee S, Sjostedt E, Fagerberg L, Bidkhori G, et al. A pathology atlas of the human cancer transcriptome. Science. 2017;357(6352). doi: 10.1126/science.aan2507 PMID: 28818916.

19. Kong Y, Yu T. A graph-embedded deep feedforward network for disease outcome classification and feature selection using gene expression data. Bioinformatics. 2018;34(21):3727-3737. doi: 10.1093/bioinformatics/bty429 PMID: 29850911.

20. Wei L, Jin Z, Yang S, Xu Y, Zhu Y, Ji Y. TCGA-assembler 2: software pipeline for retrieval and processing of TCGA/CPTAC data. Bioinformatics. 2018;34(9):1615-1617. doi: 10.1093/bioinformatics/btx812 PMID: 29272348.

21. Champion M, Brennan K, Croonenborghs T, Gentles AJ, Pochet N, Gevaert O. Module Analysis Captures Pancancer Genetically and Epigenetically Deregulated Cancer Driver Genes for Smoking and Antiviral Response. EBioMedicine. 2018;27:156-166. doi: 10.1016/j.ebiom.2017.11.028 PMID: 29331675.

22. Friedman J, Hastie T, Tibshirani R. Regularization paths for generalized linear models via coordinate descent. Journal of statistical software. 2010;33(1):1.

Supplementary Figure 1
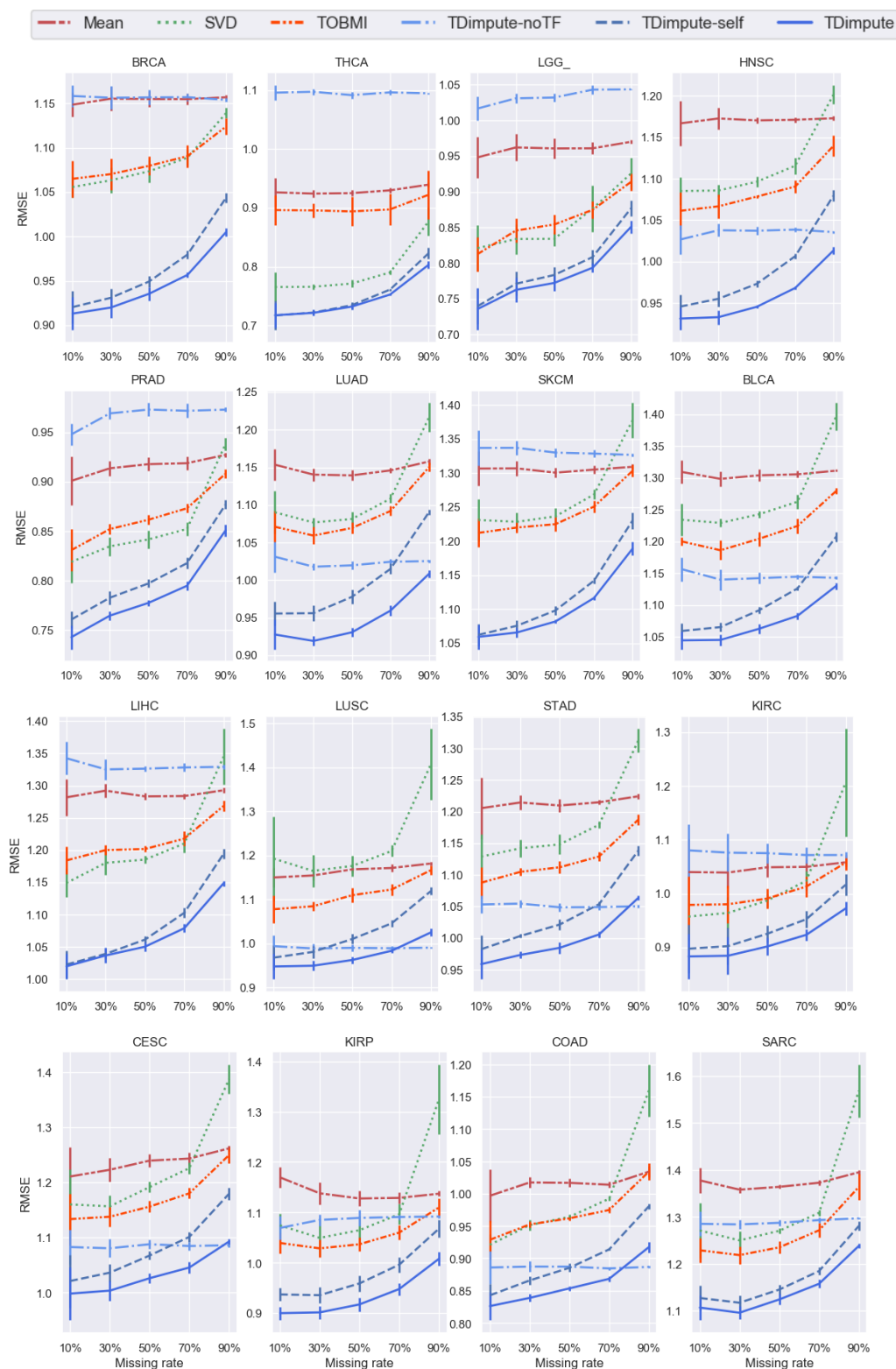
Fig S1. RMSE on 16 imputed cancer datasets with different missing rates. The results were averaged over 5 random replicas. The standard deviations are shown with error bars.

Supplementary Figure 2
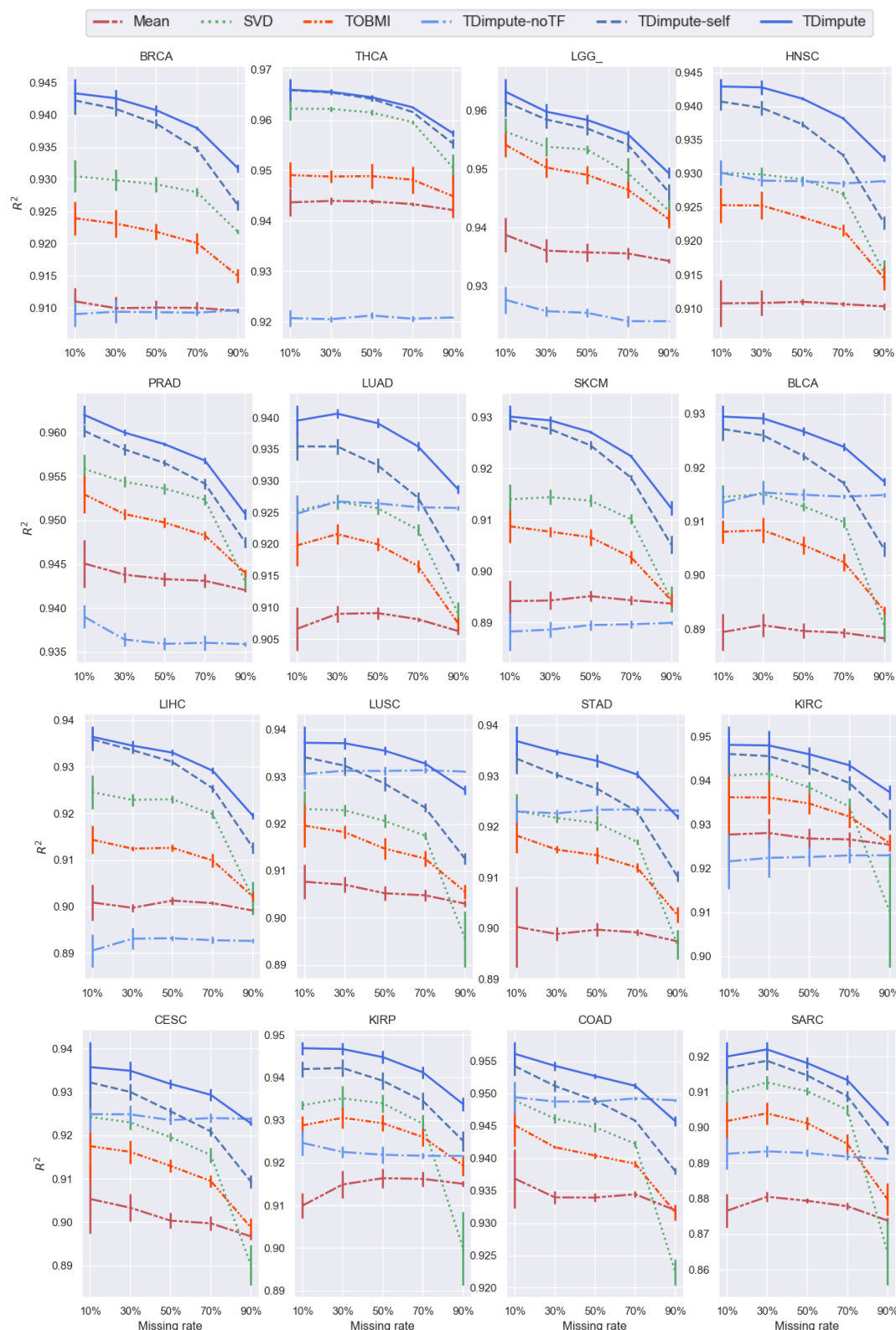
Fig S2. The squared Pearson correlation coefficients R^2 between each sample of the imputed data and the original full data on 16 imputed cancer datasets with different missing rates. The results were averaged over 5 random replicas. The standard deviations are shown with error bars.

Supplementary Figure 3
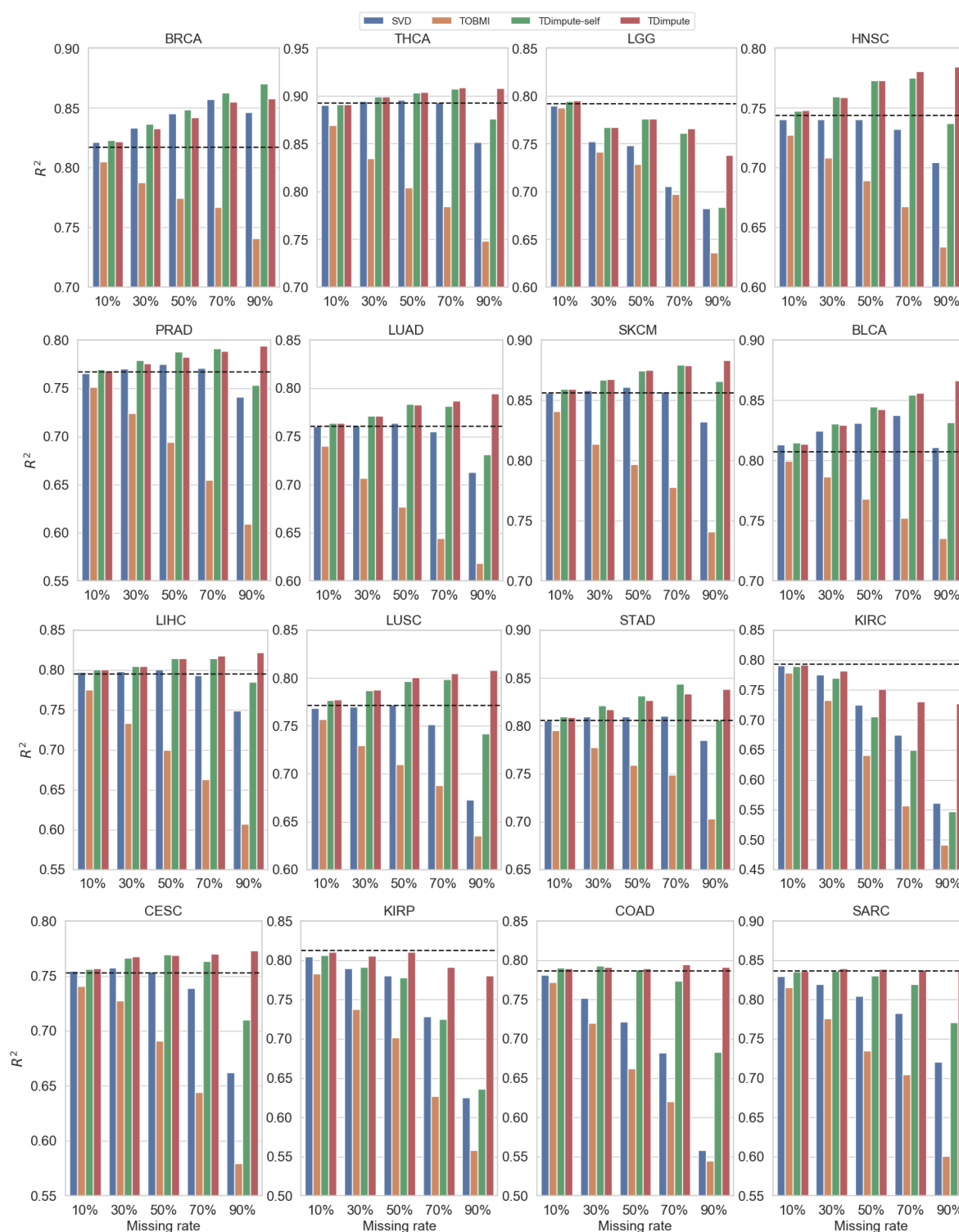
Fig S3. The squared Pearson correlation coefficients R^2 between gene expression and methylation sites on 16 imputed cancer datasets with different missing rates. The results were averaged over 5 random replicas. Dashed black line is drawn as a reference indicating the correlations from the original full dataset.

Supplementary Figure 4
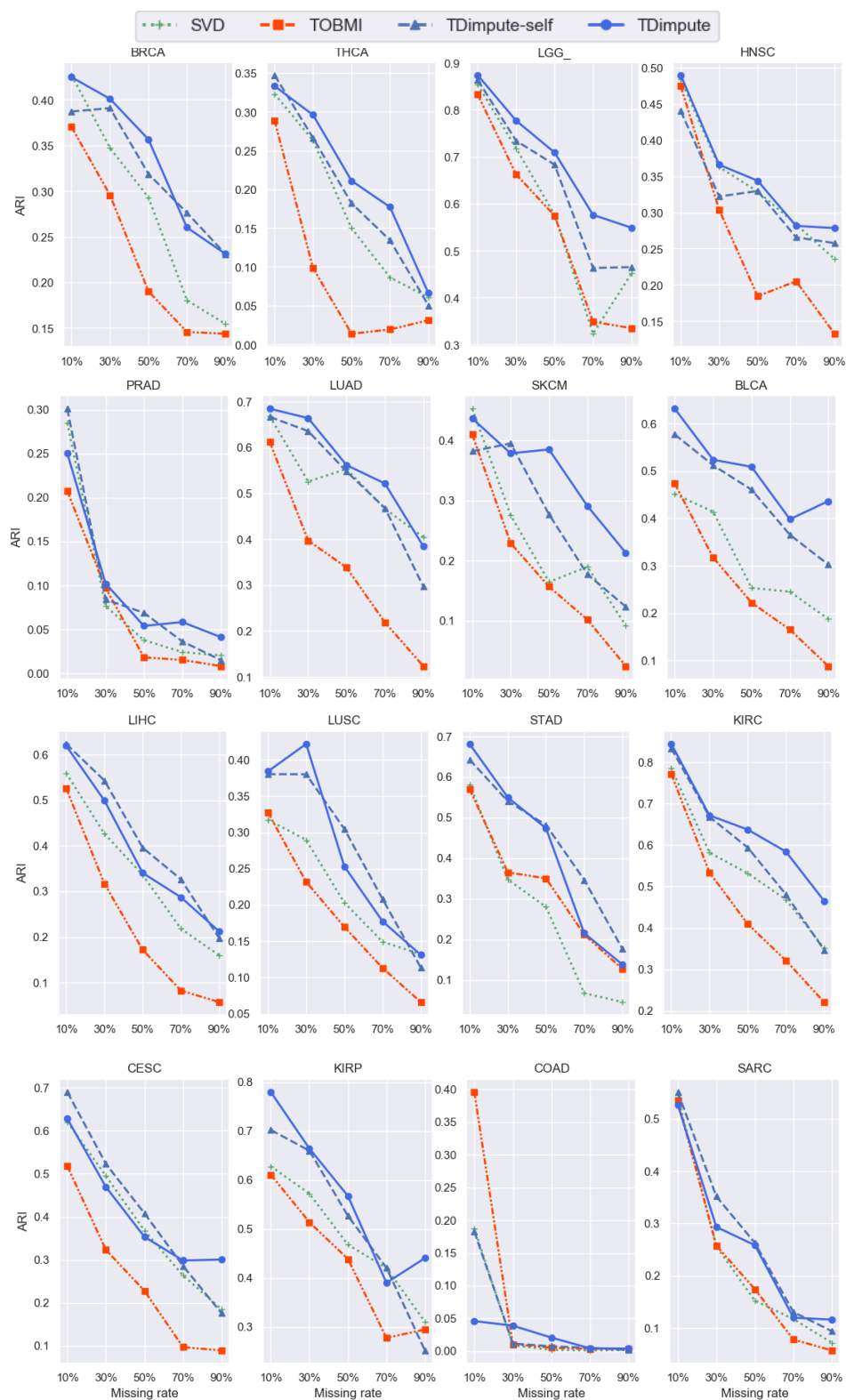
Fig S4. ARI on 16 imputed cancer datasets with different missing rates. The results were averaged over 5 random replicas.

Supplementary Figure 5
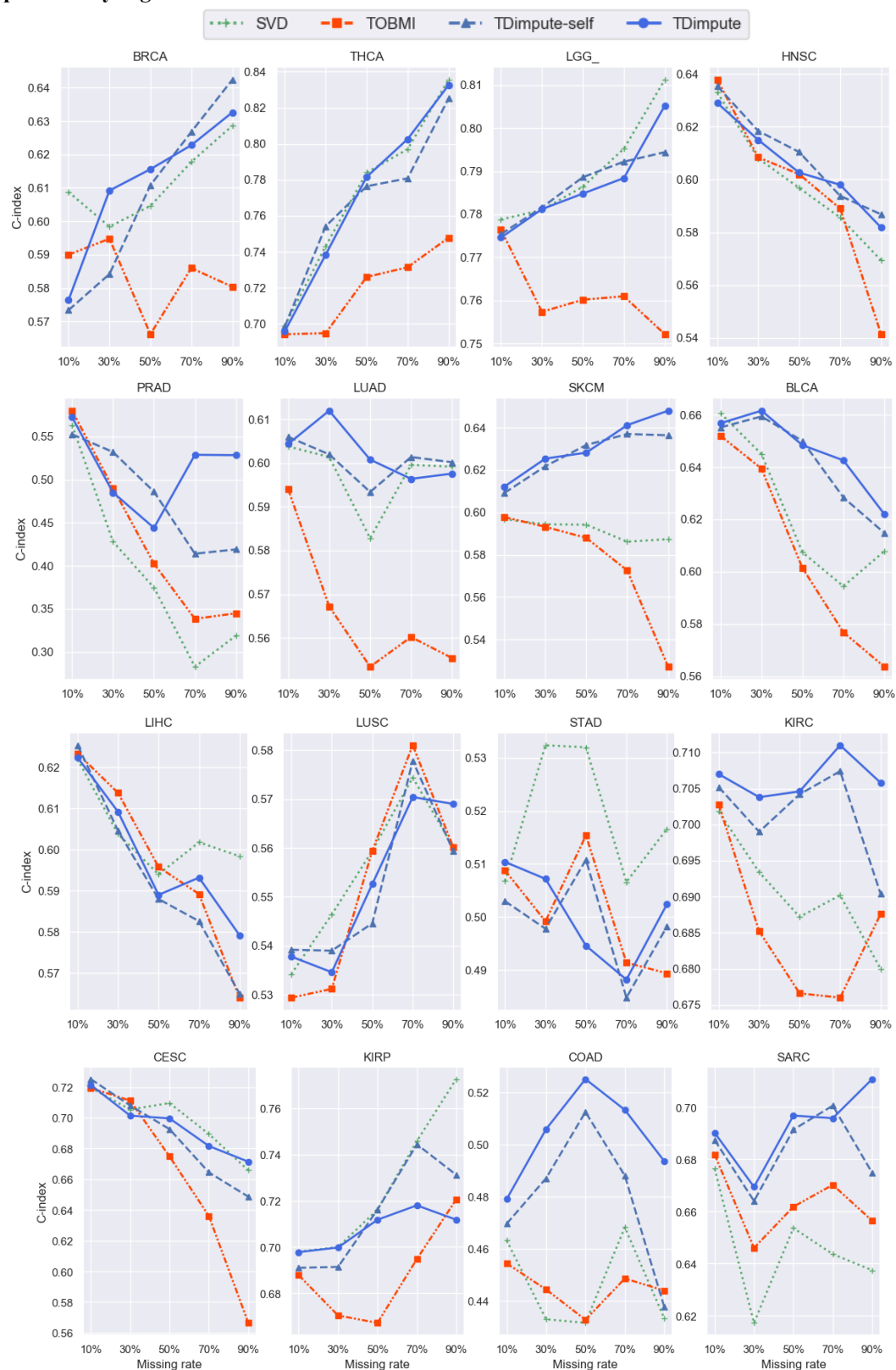
Fig S5. C-index on 16 imputed cancer datasets with different missing rates. The results were averaged over 5 random replicas.

Table S1. The TCGA cancer types and their sample sizes used for test.

Cancers	Dataset size
BRCA	867
SARC	262
LUSC	378
BLCA	424
KIRC	342
LGG_	541
PRAD	532
LUAD	477
LIHC	416
SKCM	472
HNSC	541
CESC	308
COAD	297
KIRP	297
THCA	562
STAD	371

Imputing RNA-seq data by TDimpute

Table S2. PR-AUC for detecting methylation-driving genes on imputed cancer datasets over 16 cancer types.

Missing rate	BRCA					THCA			
	SVD	TOBMI	TDimpute-self	TDimpute		SVD	TOBMI	TDimpute-self	TDimpute
10%	**1**	0.994	**1**	**1**		**0.998**	0.99	**0.998**	**0.998**
30%	0.978	0.972	0.988	**0.99**		0.98	0.97	**0.986**	**0.986**
50%	0.94	0.926	0.97	**0.97**		0.96	0.92	**0.964**	**0.964**
70%	0.872	0.862	0.932	**0.94**		0.926	0.854	0.932	**0.934**
90%	0.76	0.736	0.826	**0.854**		0.828	0.754	0.84	**0.856**

Missing rate	PRAD					LUAD			
	SVD	TOBMI	TDimpute-self	TDimpute		SVD	TOBMI	TDimpute-self	TDimpute
10%	0.994	0.992	**0.996**	0.996		0.982	0.986	**0.99**	**0.99**
30%	0.978	0.974	0.98	**0.984**		0.93	0.95	0.956	**0.964**
50%	0.946	0.93	0.958	**0.962**		0.86	0.89	0.908	**0.928**
70%	0.9	0.834	0.918	**0.926**		0.76	0.782	0.812	**0.85**
90%	0.768	0.676	0.792	**0.838**		0.554	0.602	0.606	**0.714**

Missing rate	LIHC					LUSC			
	SVD	TOBMI	TDimpute-self	TDimpute		SVD	TOBMI	TDimpute-self	TDimpute
10%	**0.99**	**0.99**	**0.99**	**0.99**		0.978	0.986	**0.99**	**0.99**
30%	0.954	0.95	0.968	**0.97**		0.92	0.948	0.96	**0.964**
50%	0.904	0.896	0.928	**0.936**		0.846	0.874	0.906	**0.928**
70%	0.836	0.814	0.866	**0.882**		0.73	0.77	0.824	**0.862**
90%	0.686	0.646	0.728	**0.774**		0.522	0.572	0.648	**0.738**

Missing rate	CESC					KIRP			
	SVD	TOBMI	TDimpute-self	TDimpute		SVD	TOBMI	TDimpute-self	TDimpute
10%	0.986	**0.988**	**0.988**	0.988		0.968	0.97	0.98	**0.984**
30%	0.94	0.944	0.96	**0.966**		0.92	0.924	0.942	**0.952**
50%	0.87	0.876	0.91	**0.928**		0.85	0.852	0.888	**0.914**
70%	0.758	0.746	0.814	**0.856**		0.764	0.75	0.804	**0.85**
90%	0.582	0.59	0.622	**0.748**		0.616	0.602	0.642	**0.744**

Missing rate	LGG					HNSC			
	SVD	TOBMI	TDimpute-self	TDimpute		SVD	TOBMI	TDimpute-self	TDimpute
10%	0.99	0.99	0.994	**1**		0.99	0.99	0.992	**0.994**
30%	0.966	0.964	0.976	**0.98**		0.958	0.956	0.972	**0.98**
50%	0.916	0.908	0.952	**0.956**		0.89	0.888	0.94	**0.952**
70%	0.814	0.816	0.898	**0.906**		0.778	0.776	0.856	**0.896**
90%	0.714	0.676	0.722	**0.77**		0.588	0.576	0.62	**0.762**

Missing rate	SKCM					BLCA			
	SVD	TOBMI	TDimpute-self	TDimpute		SVD	TOBMI	TDimpute-self	TDimpute
10%	0.99	0.994	**0.996**	0.996		0.99	0.99	**0.992**	0.992
30%	0.964	0.97	0.98	**0.982**		0.962	0.966	0.974	**0.978**
50%	0.894	0.91	0.942	**0.952**		0.92	0.922	0.944	**0.952**
70%	0.78	0.798	0.866	**0.9**		0.86	0.862	0.896	**0.916**
90%	0.65	0.64	0.676	**0.77**		0.726	0.726	0.786	**0.838**

Missing rate	STAD					KIRC			
	SVD	TOBMI	TDimpute-self	TDimpute		SVD	TOBMI	TDimpute-self	TDimpute
10%	0.992	0.992	**0.996**	0.996		0.98	0.974	**0.986**	**0.986**
30%	0.97	0.976	0.984	**0.986**		0.928	0.898	0.938	**0.948**
50%	0.94	0.952	0.964	**0.968**		0.852	0.792	0.866	**0.892**
70%	0.894	0.91	0.934	**0.94**		0.742	0.646	0.764	**0.822**
90%	0.78	0.774	0.832	**0.866**		0.56	0.518	0.56	**0.706**

Missing rate	COAD					SARC			
	SVD	TOBMI	TDimpute-self	TDimpute		SVD	TOBMI	TDimpute-self	TDimpute
10%	0.992	0.992	0.994	**0.996**		0.98	0.988	**0.99**	**0.99**
30%	0.968	0.97	0.978	**0.98**		0.946	0.958	0.964	**0.97**
50%	0.926	0.918	0.948	**0.954**		0.892	0.912	0.926	**0.934**
70%	0.856	0.852	0.902	**0.922**		0.82	0.838	0.86	**0.876**
90%	0.642	0.674	0.764	**0.856**		0.664	0.658	0.72	**0.772**

The results are averaged over 5 random replicas. Best results are highlighted in bold face.

Zhou et al.

Table S3.1. Overlap of top 100 methylation-driving genes from imputed dataset and full dataset

Missing rate	SVD	TOBMI	TDimpute-self	TDimpute
10%	89.61[*]	87.66[*]	91.59	**91.98**
30%	76.03[*]	71.83[*]	83.14[*]	**84.00**
50%	62.44[*]	55.21[*]	73.09[*]	**76.24**
70%	45.43[*]	37.70[*]	57.96[*]	**65.66**
90%	24.83	18.48[*]	26.73[*]	**50.43**

The results are averaged over 5 random replicas. Best results are highlighted in bold face. * indicates statistical significance (p-value < 0.05) between TDimpute and other three methods (SVD, TOBMI, TDimpute-self).

Table S3.2. Overlap of top 100 methylation-driving genes between imputed dataset and full dataset over 16 cancer types

Missing rate	BRCA SVD	TOBMI	TDimpute-self	TDimpute		THCA SVD	TOBMI	TDimpute-self	TDimpute
10%	96.2	93	95.8	**95.2**		**97.6**	96	97.4	**97.6**
30%	93.2	82.8	92.2	**93.4**		94	87.2	**94.8**	94.2
50%	86.8	69.4	**90.4**	88.8		88	68.2	89.8	**90.8**
70%	73.6	44	81.6	**85.8**		75.6	57.6	83.2	**85.4**
90%	34.6	9.6	45.6	**66.2**		34.2	31.6	52.4	**71**

Missing rate	PRAD SVD	TOBMI	TDimpute-self	TDimpute		LUAD SVD	TOBMI	TDimpute-self	TDimpute
10%	84.4	81	89	**90.2**		93.8	92.4	**94.6**	93.8
30%	61.8	59.4	**78.8**	77.4		84.4	82.4	87.2	**87.6**
50%	48.4	47.8	**66.2**	64.4		77.8	73.2	82.2	**83.6**
70%	38.6	37	51.2	**52.6**		63.8	63.4	73.8	**77.8**
90%	26.2	21.8	26.2	**36**		40.2	38.6	38.6	**68.4**

Missing rate	LIHC SVD	TOBMI	TDimpute-self	TDimpute		LUSC SVD	TOBMI	TDimpute-self	TDimpute
10%	85.6	87.2	91.4	**92**		94.6	93.2	94	**95.4**
30%	72.6	72.4	80.6	**81.6**		86.4	83.4	**89.6**	89
50%	64.8	53.2	72.4	**76.2**		75.6	71	82.6	**83.8**
70%	50	25.2	56.6	**60**		51.4	46.2	75.2	**78.4**
90%	27.4	8.2	31	**51.2**		18.2	16.2	23.2	**65**

Missing rate	CESC SVD	TOBMI	TDimpute-self	TDimpute		KIRP SVD	TOBMI	TDimpute-self	TDimpute
10%	89.2	82.4	**91**	90.2		83.2	79.4	84.8	**87.2**
30%	73.2	64.2	78.8	**82.2**		68.4	57.8	74	**78.2**
50%	47	40.8	57.6	**70.4**		53.2	45	59.6	**67**
70%	30.4	30.6	33.2	**54.2**		37.6	22.8	42.8	**54**
90%	18.2	16.4	17.8	**38.4**		16.2	10.6	12	**36.6**

Missing rate	LGG SVD	TOBMI	TDimpute-self	TDimpute		HNSC SVD	TOBMI	TDimpute-self	TDimpute
10%	81.6	81.8	88.4	**89.8**		91.6	90.6	**92.2**	92
30%	67.2	63.6	75.8	**79.2**		80	79.8	**84.6**	83.4
50%	59.8	57.4	64	**67.6**		66.2	66.6	77.6	**80.4**
70%	48.2	45.2	52.2	**53**		42.6	52.6	65.6	**72.8**
90%	33.2	21.4	26.4	**34.6**		18.2	30.6	22.2	**58.2**

Missing rate	SKCM SVD	TOBMI	TDimpute-self	TDimpute		BLCA SVD	TOBMI	TDimpute-self	TDimpute
10%	95.6	94.8	**96.4**	**96.4**		94.4	92.2	**95**	94.6
30%	86.2	83.6	91.4	**92.6**		85.6	78.6	**90.2**	90
50%	78.4	72	86.4	**89.6**		72	55.8	85.6	**86.8**
70%	60.4	47.2	71	**78.4**		51	36.2	72.2	**80**
90%	36	24.4	43.8	**64.2**		33.4	23.8	29.8	**67**

Missing rate	STAD SVD	TOBMI	TDimpute-self	TDimpute		KIRC SVD	TOBMI	TDimpute-self	TDimpute
10%	84.4	84.2	**87.4**	**87.4**		88.4	85.2	89.6	**91**
30%	69.4	69.8	**81**	79		71.4	66.6	74.8	**77.8**
50%	54.4	55.6	**69.4**	68.8		55.4	47.4	60.8	**65.6**
70%	36.4	41.6	55.2	**61.6**		36.8	30.8	45.4	**54**
90%	19.4	15.2	25.8	**44**		24.2	19.8	13.2	**39.2**

Missing rate	COAD SVD	TOBMI	TDimpute-self	TDimpute		SARC SVD	TOBMI	TDimpute-self	TDimpute
10%	83.4	81.4	**86.8**	86.4		89.8	87.8	91.6	**92.4**
30%	47.6	55	71.4	**72**		75	62.6	85	**86.4**
50%	19	31.2	54.8	**60.4**		52.2	28.8	70	**75.6**
70%	5.4	12.6	27.4	**42.6**		25	10.2	40.8	**60**
90%	3.4	2	1.2	**23.8**		14.2	5.4	18.4	**43**

The results are averaged over 5 random replicas. Best results are highlighted in bold face.

Imputing RNA-seq data by TDimpute

Table S4. PR-AUC for detecting significantly prognostic gene on imputed datasets over 16 cancer types.

Missing rate	BRCA					THCA			
	SVD	TOBMI	TDimpute-self	TDimpute		SVD	TOBMI	TDimpute-self	TDimpute
10%	0.892	0.918	0.932	**0.938**		0.878	0.884	0.9	**0.906**
30%	0.738	0.82	0.844	**0.852**		0.658	0.642	0.714	**0.718**
50%	0.548	0.664	0.71	**0.736**		0.466	0.498	0.556	**0.588**
70%	0.382	0.446	0.526	**0.542**		0.344	0.352	0.42	**0.468**
90%	0.306	0.358	0.376	**0.406**		0.184	0.166	0.178	**0.238**
Missing rate	PRAD					LUAD			
	SVD	TOBMI	TDimpute-self	TDimpute		SVD	TOBMI	TDimpute-self	TDimpute
10%	**0.936**	**0.936**	0.924	0.936		0.936	0.94	0.952	**0.952**
30%	0.65	0.648	0.638	**0.67**		0.814	0.846	0.87	**0.882**
50%	0.42	0.432	0.43	**0.46**		0.676	0.706	0.748	**0.764**
70%	0.294	0.3	0.3	**0.316**		0.536	0.564	0.596	**0.654**
90%	0.104	0.092	0.104	**0.122**		0.36	0.402	0.398	**0.504**
Missing rate	LIHC					LUSC			
	SVD	TOBMI	TDimpute-self	TDimpute		SVD	TOBMI	TDimpute-self	TDimpute
10%	0.84	0.832	0.856	**0.866**		0.822	0.838	**0.864**	0.86
30%	0.614	0.648	0.676	**0.704**		0.556	0.544	0.574	**0.602**
50%	0.44	0.476	0.508	**0.524**		0.376	0.346	0.4	**0.43**
70%	0.288	0.308	0.356	**0.418**		0.22	0.21	0.236	**0.27**
90%	0.162	0.146	0.178	**0.248**		0.122	0.106	0.132	**0.178**
Missing rate	CESC					KIRP			
	SVD	TOBMI	TDimpute-self	TDimpute		SVD	TOBMI	TDimpute-self	TDimpute
10%	0.932	0.938	0.946	**0.948**		0.938	0.956	0.956	**0.96**
30%	0.802	0.816	0.828	**0.842**		0.812	0.864	0.866	**0.884**
50%	0.662	0.666	0.694	**0.708**		0.752	0.754	0.758	**0.78**
70%	0.47	0.438	0.516	**0.534**		0.582	0.642	0.608	**0.658**
90%	0.26	0.23	0.27	**0.378**		0.352	0.386	0.376	**0.452**
Missing rate	LGG					HNSC			
	SVD	TOBMI	TDimpute-self	TDimpute		SVD	TOBMI	TDimpute-self	TDimpute
10%	0.988	0.99	**0.992**	0.992		0.922	0.944	0.948	**0.952**
30%	0.964	0.966	0.97	**0.97**		0.754	0.82	0.83	**0.84**
50%	0.926	0.924	0.932	**0.938**		0.572	0.66	0.688	**0.728**
70%	0.872	0.868	0.878	**0.886**		0.448	0.496	0.518	**0.57**
90%	0.796	0.728	0.756	**0.79**		0.292	0.268	0.31	**0.418**
Missing rate	SKCM					BLCA			
	SVD	TOBMI	TDimpute-self	TDimpute		SVD	TOBMI	TDimpute-self	TDimpute
10%	**0.184**	**0.184**	**0.184**	0.182		0.866	0.91	0.922	**0.926**
30%	0.182	**0.184**	0.182	0.182		0.592	0.732	0.764	**0.778**
50%	**0.188**	**0.188**	0.182	0.182		0.462	0.562	0.652	**0.68**
70%	**0.188**	**0.188**	0.182	0.18		0.342	0.412	0.496	**0.554**
90%	0.198	**0.202**	0.192	0.184		0.238	0.218	0.292	**0.424**
Missing rate	STAD					KIRC			
	SVD	TOBMI	TDimpute-self	TDimpute		SVD	TOBMI	TDimpute-self	TDimpute
10%	0.876	0.862	0.884	**0.886**		0.984	0.99	0.99	**0.992**
30%	0.544	0.6	0.65	**0.656**		0.944	0.962	0.966	**0.968**
50%	0.372	0.424	**0.46**	0.454		0.898	0.918	0.934	**0.938**
70%	0.158	0.224	0.246	**0.248**		0.802	0.84	0.872	**0.882**
90%	0.078	0.112	0.116	**0.132**		0.648	0.674	0.664	**0.726**
Missing rate	COAD					SARC			
	SVD	TOBMI	TDimpute-self	TDimpute		SVD	TOBMI	TDimpute-self	TDimpute
10%	0.778	0.804	0.824	**0.836**		0.926	0.936	0.94	**0.942**
30%	0.42	0.458	0.462	**0.512**		0.738	0.79	0.8	**0.816**
50%	0.202	0.228	0.23	**0.298**		0.552	0.614	0.618	**0.658**
70%	0.118	0.122	0.136	**0.194**		0.424	0.454	0.472	**0.528**
90%	0.058	0.058	0.064	**0.106**		0.246	0.29	0.316	**0.398**

The results are averaged over 5 random replicas. Best results are highlighted in bold face.

Zhou et al.

Table S5.1. Overlap of top 100 significantly prognostic genes identified by univariate Cox model between imputed datasets and full datasets.

Missing rate	SVD	TOBMI	TDimpute-self	TDimpute
10%	73.5*	74.8*	76.4*	**77.5**
30%	50.6*	52.3*	56.6	**57.3**
50%	37.6*	37.8*	44.2	**44.9**
70%	27.3*	26.6*	33.2*	**35.2**
90%	15.8*	16*	20.6*	**24.6**

The results are averaged over 5 random replicas. Best results are highlighted in bold face. * indicates statistical significance (p-value < 0.05) between TDimpute and other three methods (SVD, TOBMI, TDimpute-self).

Table S5.2. Overlap of top 100 prognostic genes identified by univariate Cox model between imputed dataset and full dataset over 16 cancer types.

Missing rate	BRCA					THCA			
	SVD	TOBMI	TDimpute-self	TDimpute		SVD	TOBMI	TDimpute-self	TDimpute
10%	63.4	70	**73**	72.4		69.2	68.2	70.2	**70.6**
30%	40.6	52.2	52.8	**54.8**		46	42.2	**49.4**	49
50%	27.2	33.8	36.2	**39.4**		31.2	28.2	33.4	**35.2**
70%	13.8	18	21.2	**24**		22.2	18.4	**25.2**	23.8
90%	6.2	5.8	9.4	**12.6**		**16.4**	8	12.8	15.4
Missing rate	PRAD					LUAD			
	SVD	TOBMI	TDimpute-self	TDimpute		SVD	TOBMI	TDimpute-self	TDimpute
10%	86	85.4	83.4	**85.6**		75.8	76.6	79.8	**82.8**
30%	51.4	49.2	52	**54.6**		58	53.8	**66**	64
50%	29.4	29	32.6	**33.4**		48	41.4	51.8	**53**
70%	18.6	19	19	**19.4**		33.2	27	37.8	**47.2**
90%	2.8	3.4	3.6	**4.4**		19.4	9.8	21	**32**
Missing rate	LIHC					LUSC			
	SVD	TOBMI	TDimpute-self	TDimpute		SVD	TOBMI	TDimpute-self	TDimpute
10%	65	64.2	67.8	**68**		59.8	63	63.4	**68.8**
30%	45.2	48	**53.2**	50.2		32.6	35.4	**38.6**	**38.6**
50%	29.8	32.2	**37**	34.2		20.4	20.2	23.6	**24.8**
70%	**23.2**	19	21.4	22.2		10.4	9.4	11	**14.2**
90%	7.2	4.6	8	**13**		2.2	2	2.8	**6**
Missing rate	CESC					KIRP			
	SVD	TOBMI	TDimpute-self	TDimpute		SVD	TOBMI	TDimpute-self	TDimpute
10%	81.6	79.6	80.2	**82.2**		88.6	87.8	87.8	**88.8**
30%	58.8	60.4	59	**63.6**		**85.2**	68	85	81
50%	43.6	47.2	48.4	**50.4**		**83.8**	55.6	82.2	77.6
70%	21.2	21.4	**31.2**	30.2		80.2	57.4	**83.2**	82
90%	4.4	5.4	8.4	**13**		49.4	49.6	59.4	**67.4**
Missing rate	LGG					HNSC			
	SVD	TOBMI	TDimpute-self	TDimpute		SVD	TOBMI	TDimpute-self	TDimpute
10%	90.2	89.6	91.2	**92.6**		69	70.6	**77.2**	**77.2**
30%	87.4	87.2	**88.6**	88		47	50.4	52.2	**56**
50%	88	86.4	**89**	88		28.2	33.6	37.6	**42.4**
70%	84.4	90.4	90.6	**91.2**		16.4	18.8	22.2	**28.4**
90%	80.8	85.4	**92.6**	90		6.4	3.6	7.2	**13.8**
Missing rate	SKCM					BLCA			
	SVD	TOBMI	TDimpute-self	TDimpute		SVD	TOBMI	TDimpute-self	TDimpute
10%	61	66.2	**66.4**	65.2		69.4	74.6	74.8	**75.6**
30%	30.2	37.2	37.4	**39.2**		37.6	47.6	**54.6**	54.2
50%	11.8	15.2	**21**	20.4		21.2	26.8	**41.8**	41.6
70%	3.2	6.2	8.6	**11.8**		14.6	15.2	27.2	**31.8**
90%	1.8	0.4	1.4	**4.4**		7.8	4.6	10.2	**20.6**
Missing rate	STAD					KIRC			
	SVD	TOBMI	TDimpute-self	TDimpute		SVD	TOBMI	TDimpute-self	TDimpute
10%	71.6	70.2	72.2	**73**		91.4	89.6	**91.4**	91.2
30%	37.8	42.4	44.4	**45.2**		75.8	72.6	81.8	**83.2**
50%	25.4	26.4	25.8	**29.6**		65.4	64.4	**81.2**	78.2
70%	8.2	9.4	12.2	**12.6**		57.8	58.6	**76.6**	72.4
90%	**3.8**	3.4	3.2	3.6		38.6	49.8	**63.6**	62
Missing rate	COAD					SARC			
	SVD	TOBMI	TDimpute-self	TDimpute		SVD	TOBMI	TDimpute-self	TDimpute
10%	59.8	63.4	64.8	**65.6**		73.4	77	79.4	**79.6**
30%	30.4	33	32.8	**37.8**		45.8	57.2	57.8	**58**
50%	18.4	**21**	19.2	20.6		30	43	46	**49**
70%	7.8	6.6	9.2	**15**		20.8	30	35.2	**37.2**
90%	2	2.4	2.4	**8.2**		3.2	18.2	23.2	**27**

The results are averaged over 5 random replicas. Best results are highlighted in bold face.

Imputing RNA-seq data by TDimpute

Table S6. The enrichment factors of the top 100 ranked genes in the gene list from The Human Protein Atlas across 16 cancer types

Missing rate	BRCA					THCA			
	SVD	TOBMI	TDimpute-self	TDimpute		SVD	TOBMI	TDimpute-self	TDimpute
10%	7.637	8.625	8.493	**8.888**		8.664	**9.102**	8.554	**9.102**
30%	4.411	**6.584**	6.452	6.386		5.045	6.251	**6.799**	6.361
50%	2.765	4.740	**5.267**	**5.267**		3.400	4.058	**4.496**	**4.496**
70%	1.383	2.436	3.226	**3.424**		2.303	2.961	**3.509**	2.522
90%	0.790	0.988	1.580	**1.843**		1.755	1.206	**2.303**	1.864

Missing rate	PRAD					LUAD			
	SVD	TOBMI	TDimpute-self	TDimpute		SVD	TOBMI	TDimpute-self	TDimpute
10%	14.60	**15.08**	13.40	14.12		8.476	8.476	**8.944**	**8.944**
30%	8.86	**9.57**	8.86	8.14		6.839	6.079	**7.541**	**7.541**
50%	4.31	**5.74**	4.55	4.55		5.436	4.618	5.904	**5.962**
70%	3.11	**4.79**	3.59	2.15		3.566	2.923	4.150	**5.904**
90%	0.96	1.68	**2.15**	1.44		2.455	0.877	2.747	**4.092**

Missing rate	LGG					HNSC			
	SVD	TOBMI	TDimpute-self	TDimpute		SVD	TOBMI	TDimpute-self	TDimpute
10%	NA					6.29	6.92	**7.45**	7.40
30%						3.84	4.71	5.00	**5.53**
50%						1.97	3.32	3.80	**4.23**
70%						0.96	1.63	2.21	**2.64**
90%						0.34	0.19	0.72	**1.01**

Missing rate	SKCM					BLCA			
	SVD	TOBMI	TDimpute-self	TDimpute		SVD	TOBMI	TDimpute-self	TDimpute
10%	2.78	**3.53**	2.78	3.16		6.65	7.24	7.28	**7.56**
30%	1.11	**2.41**	2.23	1.86		3.13	4.94	**5.74**	5.71
50%	0.19	1.11	0.93	**1.49**		1.67	2.82	**4.42**	4.14
70%	0.00	0.74	0.00	**1.11**		0.91	1.57	2.79	**3.31**
90%	0.00	0.00	0.00	**0.37**		0.59	0.35	0.97	**2.26**

Missing rate	LIHC					LUSC			
	SVD	TOBMI	TDimpute-self	TDimpute		SVD	TOBMI	TDimpute-self	TDimpute
10%	1.004	0.951	1.017	**1.030**		1.403	1.637	1.578	**1.695**
30%	**0.700**	0.647	**0.700**	0.674		0.760	1.169	1.286	**1.461**
50%	0.396	**0.449**	0.436	0.370		0.526	0.760	0.701	**0.818**
70%	**0.304**	0.225	0.225	0.277		0.292	**0.526**	0.292	0.468
90%	**0.119**	0.000	0.092	**0.119**		0.000	**0.058**	0.000	**0.058**

Missing rate	CESC					KIRP			
	SVD	TOBMI	TDimpute-self	TDimpute		SVD	TOBMI	TDimpute-self	TDimpute
10%	13.09	13.19	13.19	**13.51**		0.363	0.363	**0.370**	0.363
30%	9.62	10.62	10.04	**10.83**		**0.351**	0.287	**0.351**	0.332
50%	6.73	8.15	7.99	**8.83**		**0.370**	0.236	**0.370**	0.338
70%	2.58	3.68	4.73	**5.10**		0.332	0.300	**0.363**	0.338
90%	0.47	0.68	1.31	**2.05**		0.217	0.217	0.255	**0.281**

Missing rate	STAD					KIRC			
	SVD	TOBMI	TDimpute-self	TDimpute		SVD	TOBMI	TDimpute-self	TDimpute
10%	5.09	5.09	**5.47**	5.35		0.281	0.281	**0.287**	**0.287**
30%	2.80	2.80	3.18	**3.69**		0.255	0.261	0.255	**0.268**
50%	0.89	1.65	1.53	**1.78**		0.210	0.223	0.268	**0.274**
70%	0.00	0.38	**0.89**	0.76		0.185	0.204	0.249	**0.268**
90%	0.00	0.13	0.00	**0.25**		0.096	0.185	0.217	**0.236**

Missing rate	COAD					SARC			
	SVD	TOBMI	TDimpute-self	TDimpute		SVD	TOBMI	TDimpute-self	TDimpute
10%	1.02	1.09	1.15	**1.28**		NA			
30%	0.77	**0.83**	0.70	0.77					
50%	0.32	0.45	**0.51**	0.32					
70%	0.00	0.00	0.00	**0.19**					
90%	0.06	0.06	0.06	**0.13**					

The results are averaged over 5 random replicas. Best results are highlighted in bold face. 'NA' means that the cancer is not included in The Human Prote

Table S7. The 26 genes validated in The Human Protein Atlas.

Gene	cancer reported in literature	Reference
SAMM50		
POLR1B	epithelial ovarian cancer	Wei L, Xin C, Wang W, et al. Microarray analysis of obese women with polycystic ovary syndrome for key gene screening, key pathway identification and drug prediction[J]. Gene, 2018, 661: 85-94.
ANKRD54		
C9orf103	acute myeloid leukemia	Sweetser D A, Peniket A J, Haaland C, et al. Delineation of the minimal commonly deleted segment and identification of candidate tumor-suppressor genes in del (9q) acute myeloid leukemia[J]. Genes, Chromosomes and Cancer, 2005, 44(3): 279-291.
SGSM3	breast cancer	Tan T, Zhang K, Sun W C. Genetic variants of ESR1 and SGSM3 are associated with the susceptibility of breast cancer in the Chinese population[J]. Breast Cancer, 2017, 24(3): 369-374.
TXN	endometrial cancer	Simmons D G, Kennedy T G. Rat endometrial Vdup1 expression: changes related to sensitization for the decidual cell reaction and hormonal control[J]. Reproduction, 2004, 127(4): 475-482.
FAM189B		
ASAP1	cervical cancer	Guo L, Lu W, Zhang X, et al. Metastasis-associated colon cancer-1 is a novel prognostic marker for cervical cancer[J]. International journal of clinical and experimental pathology, 2014, 7(7): 4150.
IRAK4	breast cancer	Perrott K M, Wiley C D, Desprez P Y, et al. Apigenin suppresses the senescence-associated secretory phenotype and paracrine effects on breast cancer cells[J]. Geroscience, 2017, 39(2): 161-173.
RILPL2	breast cancer	Chen G, Sun L, Han J, et al. RILPL2 regulates breast cancer proliferation, metastasis, and chemoresistance via the TUBB3/PTEN pathway[J]. American journal of cancer research, 2019, 9(8): 1583.
USP36	Neuroblastoma	Mondal T, Juvvuna P K, Kirkeby A, et al. Sense-antisense lncRNA pair encoded by locus 6p22. 3 determines neuroblastoma susceptibility via the USP36-CHD7-SOX9 regulatory axis[J]. Cancer Cell, 2018, 33(3): 417-434. e7.
RPS6KA1	prostate cancer	Yu G, Lee Y C, Cheng C J, et al. RSK promotes prostate cancer progression in bone through ING3, CKAP2, and PTK6-mediated cell survival[J]. Molecular Cancer Research, 2015, 13(2): 348-357.
MBOAT2	pancreatic ductal adenocarcinoma	Badea L, Herlea V, Dima S O, et al. Combined gene expression analysis of whole-tissue and microdissected pancreatic ductal adenocarcinoma identifies genes specifically overexpressed in tumor epithelia[J]. Hepato-gastroenterology, 2008, 55(88): 2016.
UCHL1	endometrial cancer	Nakao K, Hirakawa T, Suwa H, et al. High Expression of Ubiquitin C-terminal Hydrolase L1 Is Associated With Poor Prognosis in Endometrial Cancer Patients[J]. International Journal of Gynecologic Cancer, 2018, 28(4): 675-683.
GAL	endometrial cancer	Mylonas I, Mayr D, Walzel H, et al. Mucin 1, Thomsen-Friedenreich expression and galectin-1 binding in endometrioid adenocarcinoma: an immunohistochemical analysis[J]. Anticancer research, 2007, 27(4A): 1975-1980.
ANKRD22	non-small cell lung cancer	Yin J, Fu W, Dai L, et al. ANKRD22 promotes progression of non-small cell lung cancer through transcriptional up-regulation of E2F1[J]. Scientific reports, 2017, 7(1): 4430.
TTLL1		
CGREF1		
CLCN4	colon cancer	Ishiguro T, Avila H, Lin S Y, et al. Gene trapping identifies chloride channel 4 as a novel inducer of colon cancer cell migration, invasion and metastases[J]. British journal of cancer, 2010, 102(4): 774.
ALDH2	esophageal cancer	Liu K, Song G, Zhu X, et al. Association between ALDH2 Glu487Lys polymorphism and the risk of esophageal cancer[J]. Medicine, 2017, 96(16).
CALCA	endometrial cancer	Andronowska A, Chruściel M, Całka J. The localization and expression of NADPH-diaphorase and isoforms of nitric oxide synthase in the porcine gravid uterus[J]. Reproductive biology, 2008, 8(3): 263-278.
CBY1	breast cancer	Glinskii A B, Glinsky G V, Lin H Y, et al. Modification of survival pathway gene expression in human breast cancer cells by tetraiodothyroacetic acid (tetrac)[J]. Cell Cycle, 2009, 8(21): 3562-3570.
PEG10	endometrial cancer	Van Der Horst P H, Wang Y, Vandenput I, et al. Progesterone inhibits epithelial-to-mesenchymal transition in endometrial cancer[J]. PLoS One, 2012, 7(1): e30840.
CISH		
LMO3	gastric cancer	Qiu Y S, Jiang N N, Zhou Y, et al. LMO3 promotes gastric cancer cell invasion and proliferation through Akt-mTOR and Akt-GSK3β signaling[J]. International journal of molecular medicine, 2018, 41(5): 2755-2763.
MAFG	Liver cancer	Liu T, Yang H, Fan W, et al. Mechanisms of MAFG dysregulation in cholestatic liver injury and development of liver cancer[J]. Gastroenterology, 2018, 155(2): 557-571. e14.

Imputing RNA-seq data by TDimpute

Imputing RNA-seq data by TDimpute